Study of the Surface and Dimensional Quality of the AlSi10Mg Thin-Wall Components Manufactured by Selective Laser Melting

Muhammad Waqas [1], **Dingyong He** [1], **Hassan Elahi** [2,*], **Saleem Riaz** [3], **Marco Eugeni** [2] **and Paolo Gaudenzi** [2]

1   Faculty of Materials and Manufacturing, Beijing University of Technology, No.100, Ping Le Yuan, Beijing 100124, China; waqasm082@yahoo.com (M.W.); dyhe@bjut.edu.cn (D.H.)
2   Department of Mechanical and Aerospace Engineering, Sapienza University of Rome, 00185 Roma, Italy; marco.eugeni@uniroma1.it (M.E.); paolo.gaudenzi@uniroma1.it (P.G.)
3   School of Automation, Northwestern Polytechnical University, Xi'an 170072, China; saleemriaznwpu@mail.nwpu.edu.cn
*   Correspondence: hassan.elahi@uniroma1.it

Abstract: Additive manufacturing (AM), a 3D printing technique that manufactures components by sequential addition of powder, has massively reshaped the manufacturing and engineering sectors from batch production to manufacturing customized, innovative, state-of-the-art, and sustainable products. Additive manufacturing of aluminum alloys by selective laser melting (SLM) is one of the latest research trends in this field due to the fact of its advantages and vast applications in manufacturing industries such as automobiles and aerospace. This paper investigated the surface and dimensional quality of SLM-built AlSi10Mg parts using a response surface method (RSM) and found the influence of the wall thickness and process parameters (i.e., laser power, scanning speed, hatch distance) on the pieces. Thin-walled test specimens of AlSi10Mg alloy were manufactured with different combinations of process parameters at three wall thicknesses: 1.0 mm, 2.0 mm, and 3.0 mm. The Minitab DOE module was used to create 27 different configurations of wall thickness and process parameters. The samples' surface roughness and dimensional accuracy were investigated, and the findings were evaluated using the ANOVA technique. The regression model and the ANOVA technique showed high precision and had a particular reference value for practical engineering applications.

Keywords: selective laser melting; AlSi10Mg; surface roughness; dimensional accuracy

1. Introduction

Additive manufacturing (AM) techniques, along with newly developed alloys and conventional manufacturing processes, possess the ability to transform the method of production of industrial products. AM methods are often mentioned as layered manufacturing, owing to the nature of the procedure which involves layer-by-layer fabrication of a part while using CAD data from a computer [1–3]. AM is a generally used term in the manufacturing industry, but autofab (auto fabrication), freeform manufacturing, powder metallurgy, stereo lithography, layer-based manufacturing, and 3D printing are also commonly used terminologies while referring to additive manufacturing [2]. In the late 1980s, manufacturing industries started using additive manufacturing techniques to produce prototypes of their products for the purpose of assessing the difficulties associated with their geometry, design, and form along with their usefulness. At the end of 1990s and in the early 2000s, due to the great improvements in the reproducibility and reliability of the method, and while referring to metallic materials, owing to the employment of high-energy density sources able to consolidate these metallic materials, application of AM techniques and 3D

printing began for the production of final products [2,4–6]. Nowadays, additive manufacturing has replaced some traditional production processes, for instance, casting and forging, especially in some specific manufacturing industries, e.g., the automotive and aerospace industries. The main factors for the adoption of AM in these industries are its advantages over conventional manufacturing process such as the high degree of freedom in design and complexity of geometry, the ability to manufacture freeform surfaces, amalgamation of many components into one-part, minimal requirement of work tools, and the ability to customize production [4,7–9]. Over the last two decades, AM has been transformed from rapid prototyping-oriented 3D printers to advanced production systems having the ability to produce fully functional components of different materials with minimal involvement of tooling. So far, the focus of research in 3D printing has been the production of parts using polymer materials, but the invention of new AM techniques, including selective laser sintering/melting, laser engineered net shaping, and electron beam melting, made it possible to manufacture metallic, ceramic, and composite parts. The automobile, aerospace, military production, and biomedical industries are leading sectors utilizing additively manufactured parts [4,9–11]. The employment of AM techniques has granted designers high freedom of design and enabled manufacturing industries to produce topologically optimized components with better strength-to-weight ratios, an essential characteristic in both automobile and aerospace designs in order to produce light-weight products. AM has enormously revolutionized the biomedical industry with customized production of prosthetic parts, dental implants, hearing aids, and orthopedic parts to suit the unique needs of an individual's physiology. AM has rapidly revamped the manufacturing process within the last ten years and produced practically functional components, making these techniques commercially popular [6,9,12].

Surface roughness is one of the most important factors when evaluating the surface quality of components, and roughness has a major impact on the mechanical properties that affect the service life of components. Therefore, the role of surface roughness in the SLM parts has been investigated by many researchers. To discover the related factors influencing surface roughness, various scientific studies have been carried out.

The effects of laser power and scan speed on the surface roughness of the printed aluminum alloy samples were investigated by Dad bakhsh et al. [13]. Calignano et al. [14] concluded that with direct metal laser sintering (DMLS), the scanning speed has a significant impact on the surface roughness. Leary [15] conducted a series of surface roughness optimizations for Ti6Al4V specimens. The effect of input LEDs on the surface roughness of aluminum alloy specimens with DMLS was studied by Mohammadi and Asgari [16], but it was confined to the construction plane. Wang et al. investigated the surface roughness of SLM-built AlSi10Mg parts and established that the surface roughness first decreases noticeably and then rises gradually with the increase in laser energy density [17]. The SLM process parameters' effect on surface roughness was studied by Tian et al., and it was observed that surface roughness increased with small hatch distances that led to the adhesion of particles on the surface. They also found that good surface quality can be achieved by better scan strategies [18]. Rakesh et al. compared the effects of argon- and nitrogen-built environments for SLM of AlSi10Mg and concluded that samples built in a nitrogen atmosphere reported smoother surfaces and better mechanical properties [19].

Han et al. [20] focused on the various process parameters that influenced dimensional accuracy and recognized that a high scan speed, resulting in high densification, can help to improve dimensional accuracy. Majeed et al. [21] studied the surface and dimensional quality of SLM-built AlSi10Mg parts and defined a set of optimal process parameters. Maamoun et al. investigated the effects of the SLM process parameters on the dimensional accuracy of the AlSi10Mg parts. The results reported a dimensional tolerance variation from an oversize of 0.15–0.195 mm [22]. Sing et al. stated that the geometrical precision of the lattice structures can be enhanced by cautious variations of the process parameters. The research concluded that laser power, as compared to layer thickness and scan speed, greatly influences the dimensional accuracy of lattice structures built by SLM [23]. The

dimensional quality of SLM- and DMLS-built internally cooled cutting tools was studied by Ghani et al. They concluded that, with respect to dimensional accuracy, the DMLS method performed better than the SLM method [24]. Fateri et al. investigated the SLM of glass, finding that both high- and low-energy intensities led to poor dimensional quality causing bulging and poor bonding, respectively. They showed that 100%-dimensional accuracy is attainable by selection of the optimal process parameters [25]. Wang et al. studied the SLS process parameters' effect on dimensional accuracy and concluded that the accuracy of SLS-built parts can be improved with a higher laser power, lower scanning speed, and maximum permissible temperature of working atmosphere [26].

It is evident from the literature that there are a number of SLM process parameters that can be controlled and varied so as to obtain the desirable surface and dimensional quality of the parts. This study aimed to investigate the effect on the surface and dimensional quality of SLM-built test specimens of various combinations of laser power, scan speed, hatch distance, and wall thicknesses.

2. Experimental Method and Procedure

2.1. Equipment and Material

To manufacture the sample under study, a gas-atomized AlSi10Mg powder material was used, which is commonly used for aluminum moldings. The powder was supplied by the PAC Corporation (USA). An SLM 280HL machine of SLM solutions was employed to produce the sample. The aluminum substrate was heated to 150 °C to avoid the thermal stresses. Prior to the start of fabrication, the AlSi10Mg powder was dried out by exposing it to a temperature of 70 °C in a drying oven for 4 h. The sieving of the powder was performed in order to filter out the particles between the size of 18–58 mm for onward production. The machine used, an SLM 280HL, was supplied with the maximum scan speed of 10 m/s and two fiber lasers each with laser power of 400 watts. Build platform used to produce samples consisted of a 280 mm × 280 mm square plate. The selection of suitable process parameters is very significant for accomplishing the best results from the SLM technique. The scan speed, hatch distance, and laser power are vital parameters in the SLM process. The almost eutectic structure of AlSi10Mg in the Al–Si phase diagram and a melting temperature of 570 °C make it one of the most suitable and widely used alloys in casting. This alloy, due to the fact of its hardness and good strength, is used for thin wall and intricate geometry components prone to high loads such as in automotive and aerospace productions [27,28]. The chemical composition of AlSi10Mg is given below in Table 1.

Table 1. Composition of AlSi10Mg alloy powder as per DIN EN 1706.

ELEMENT	Si	Fe	Cu	Mn	Mg	Zn	Ti	Al
Weight %	9–11	≤0.55	≤0.05	≤0.45	0.2–0.45	≤0.1	≤0.15	Balance

2.2. Powder Characterization

The morphology of the AlSi10Mg powder particles was examined on a scanning electron microscopy (SEM) and images were taken by a Tescan VEGA 3 LMU Scanning Electron Microscope system as shown in Figure 1. A laser particle analyzer (Beckman Coulter LS 13,320) was used to measure the size of powder particles. The powder particles' size varied from an average diameter of 25–65 μm; however, some particles also had diameters smaller and larger than the abovementioned range, having different spherical and elliptical forms. The density of the loose powder was 2.68 gm/cm^3 as per the data sheet provided by PAC Corporation.
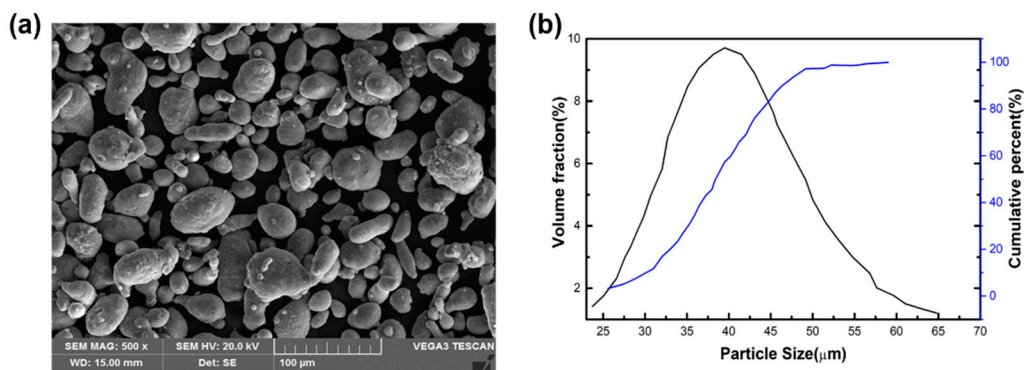
Figure 1. Morphology of AlSi10Mg; (**a**) powder particles, and (**b**) the powder size distribution.

2.3. Response Surface Methodology in Combination with Design of Experiment (DOE)

The response surface method (RSM) is a group of procedures that includes (1) outlining a group of experimentations in order to obtain trustworthy and satisfactory measurement of the response under study, (2) defining a set of the optimum process parameters that lead to the attainment of the desired value of response, and (3) explaining the influence of selected process parameters upon the response with the help of 2D and 3D plots and response surfaces. The response surface methods are categorized into three different kinds of design of experiments (DOE) techniques: (1) central composite design (CCD) was developed by Box and Wilson in 1951 and is capable of designing experimental plans up to five levels; (2) Box–Behnken design (BBD) proposed by Box and Behnken in 1960, which has the capacity to outline experimental plans up to three levels; (3) EIMSE-optimal designs presented by Allen et al. in 2003, founded on supposed "expected integrated mean squared error optimal" [29,30].

The optimization of parameters in the SLM process can be beneficial to enhance the surface and dimensional quality of fabricated parts [14,31–33]. This research aimed to undertake a comprehensive understanding of the relationship between different sets of process parameters and the surface and dimensional quality of SLM-built AlSi10Mg parts. The study, by use of optimization techniques, also tried to outline the optimized process parameters to attain better surface and dimensional quality. The main objectives of this study are as given below:

- Investigation of SLM process parameters' influence upon the surface and dimensional quality of AlSi10Mg specimens;
- To study the impact of variations of wall thickness and process parameters on surface roughness and the dimensional accuracy of the specimens;
- To determine the effect of post-processing techniques (i.e., sand blasting and polishing) on the surface and dimensional quality of the specimens;
- By using optimization techniques, to define a set of optimal process parameters against surface roughness and dimensional accuracy.

DOE by Using Minitab 17

There are many statistical software tools available for DOE and optimization purposes such as Design Expert, Statistica, Minitab, Design-Ease. Minitab 17 was used in this study for experiment planning, regression analysis, and optimization of the SLM process against surface roughness and dimensional accuracy.

This study proposes a BBD-based optimization approach. This approach, by outlining the least possible runs of experiment, suggests a set of optimum process parameters (i.e., laser power, scan speed, hatch distance) of the selective laser melting process. Response surface methods are normally applied in scenarios when the importance of some factors (process parameters) have already been established as a result of previous experimentation [29]. The DOE starts by defining the factors (in this case. the SLM process parameters)

and their levels (highs and lows). In continuation of previous research work done [34,35], three levels of four parameters (i.e., wall thickness, laser power, scan speed, and hatch spacing) were selected. The three levels of parameters employed in this study are given below in Table 2.

Table 2. Process parameters and their levels for DOE.

Parameters	Unit	Level		
		−1	0	1
Wall Thickness	mm	1.0	2.0	3.0
Laser Power	Watt	320	350	380
Scan Speed	mm/s	730	900	1070
Hatch Distance	μm	80	105	130

The powder layer thickness was kept constant at 30 μm. The experimental plan was further tested, and surface plots were produced to describe the tendency of attainable surface-roughness and dimensional accuracy against different sets of process parameters. Eventually, this is beneficial in investigating the process parameters' effect upon the subsequent responses. Moreover, it also makes us capable of defining a set of optimal process parameters with respect to dimensional accuracy and surface roughness of SLM-built AlSi10Mg specimens. The Box–Behnken design-based experimental plan generated by Minitab 17 is given below in Table 3.

Table 3. Four-factor three-level Box–Behnken DOE.

Run Order	Wall Thickness (mm)	Laser Power (Watt)	Scan Speed (mm/s)	Hatch Distance (μm)
1	1	320	900	105
2	3	320	900	105
3	1	380	900	105
4	3	380	900	105
5	2	350	730	80
6	2	350	1070	80
7	2	350	730	130
8	2	350	1070	130
9	1	350	900	80
10	3	350	900	80
11	1	350	900	130
12	3	350	900	130
13	2	320	730	105
14	2	380	730	105
15	2	320	1070	105
16	2	380	1070	105
17	1	350	730	105
18	3	350	730	105
19	1	350	1070	105
20	3	350	1070	105
21	2	320	900	80
22	2	380	900	80
23	2	320	900	130
24	2	380	900	130
25	2	350	900	105
26	2	350	900	105
27	2	350	900	105

The DOE plan consisted of 27 experimental runs with different combinations of process parameters so as to minimize the experimental cost and achieve optimization. The DOE plan does not combine all the lows or highs of all the parameters in a single run

so as to avoid extreme conditions during experimentation. Moreover, the experimental plan contains three center points, i.e., points where the middle values (0, 0, 0, 0) of all the parameters are chosen in a single run (Run 25, 26, 27). In this case, the middle values of wall thickness, laser power, scan speed, and hatch distance are 2 mm, 350 watts, 900 mm/s, and 105 μm, respectively. A center point is repeated twice to ensure the repeatability and dispersion of the experimental design.

3. Experimental Results and Analysis

3.1. Experimental Approach

In this study, two sets out of a total of 54 (27 × 02) test specimens of AlSi10Mg were manufactured using the selective laser melting technique. As mentioned earlier, Box–Behnken design, which is an RSM design, was applied to outline the experimental plan. First, a three-dimensional CAD model of the samples was prepared. The CAD model was fed into the SLM machine and the manufacturing was performed. The length (L) and height (H) of the samples were kept constant at 55 mm and 12 mm, respectively, and there were three variations in wall thickness, i.e., 1.0 mm, 2.0 mm, and 3.0 mm, against different combinations of process parameters (i.e., laser power, scan speed, hatch distance) to make 27 combinations as designed by the DOE technique. The wall thicknesses and process parameters were varied systematically to study their effects on the surface and dimensional quality of the built specimens. The specimens' dimensions and built orientation were given in Figure 2. The wall thickness (T) and length (L) of the samples were built in the horizontal direction (i.e., *x,y*-plane), while the height was built in the vertical direction, i.e., on the *z*-axis. The samples were allowed to cool down at room temperature to relieve residual stresses. Then, samples were subjected to sand blasting at a pressure of 0.3 MPa for 4 min. The wire cutting process was applied to separate specimens from the built platform and to obtain the final shape required for further tensile and hardness testing. The length and height of the samples after wire cutting were 53 mm and 10 mm, respectively. The dimensions of the final specimen after the wire cutting process are given in Figure 3. The overall flow of the manufacturing process is given in Figure 4.
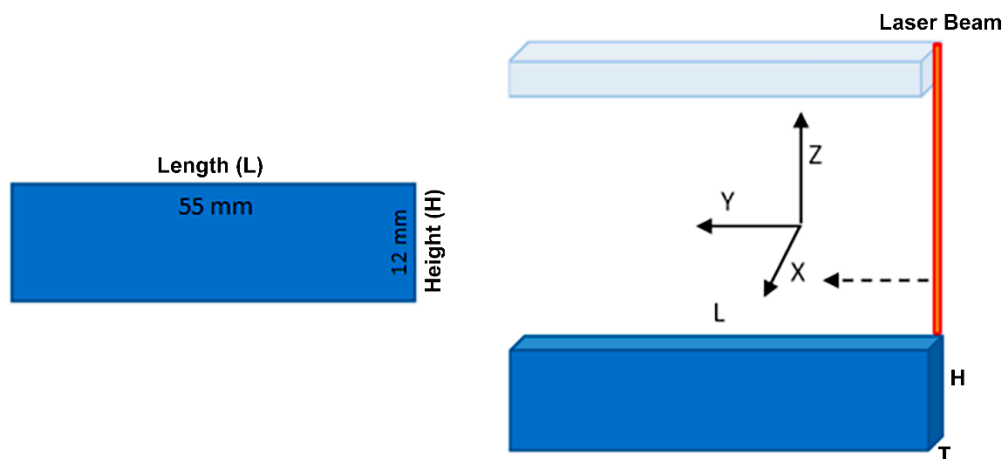

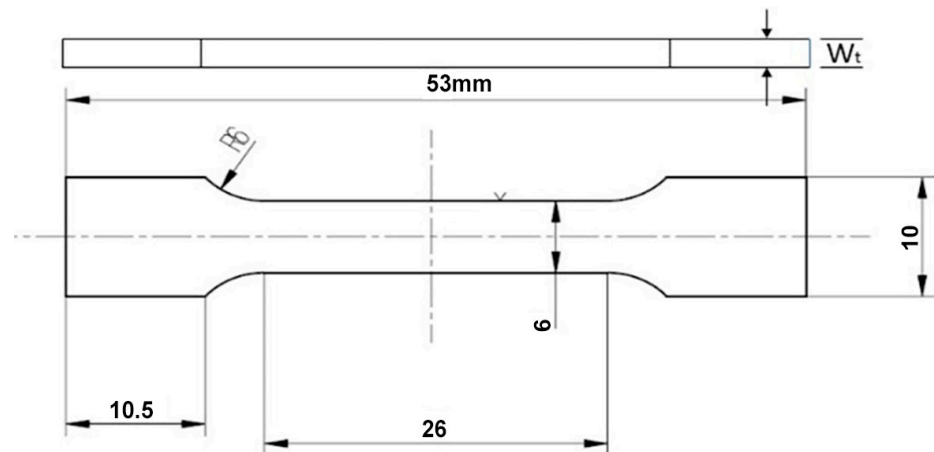**Figure 2.** Samples dimensions and built-up scheme.

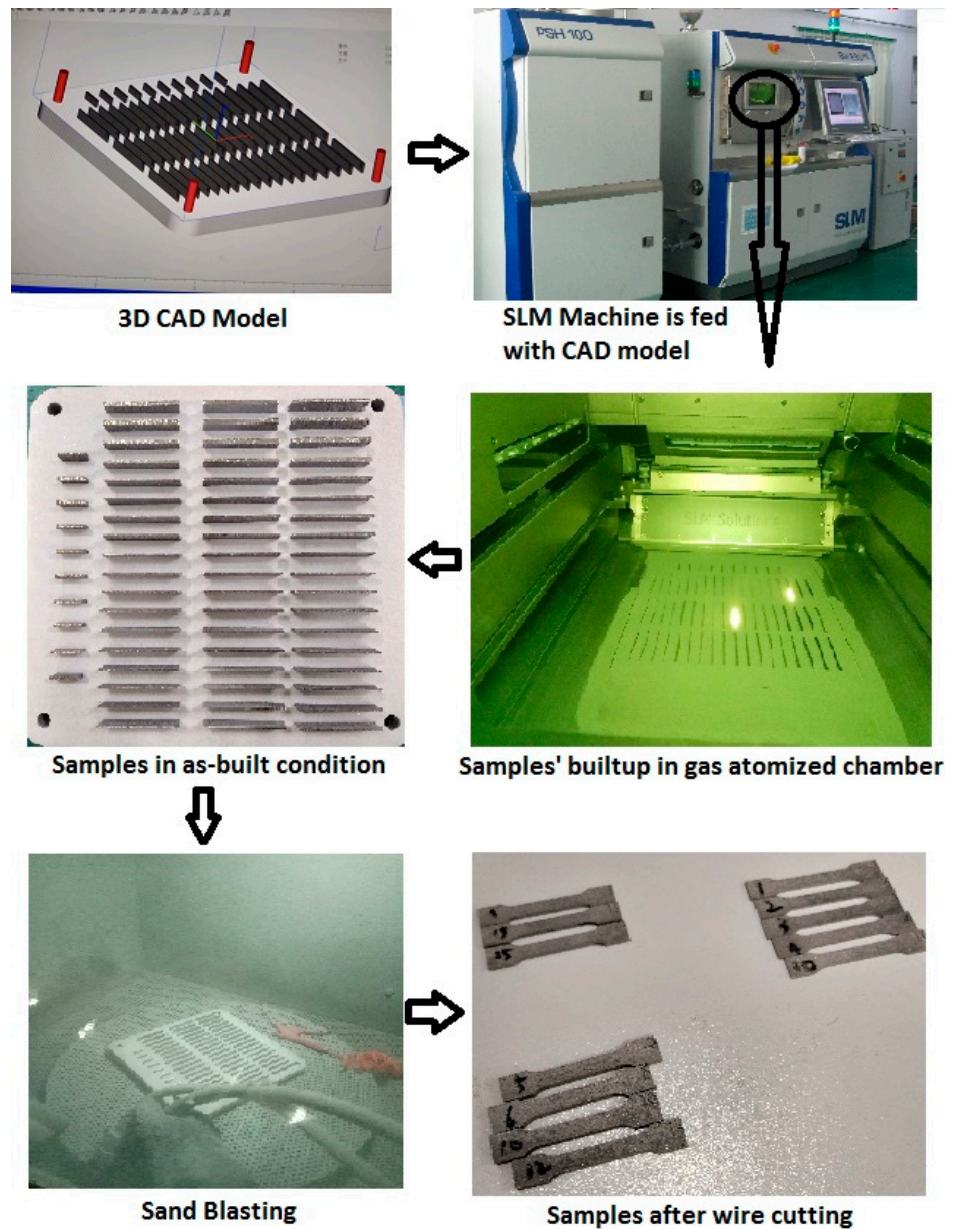**Figure 3.** Dimensions of the sample after wire cutting.

Figure 4. Overall flow of the manufacturing process.

3.2. Surface Roughness of as-Built Samples

The purpose of experimentation, as stated earlier, was to optimize the process parameters of the SLM process to improve the surface quality of AlSi10Mg parts. The samples' surface roughness was recorded using the contact method. A profilometer was used to take a reading of the sample's SR. The profilometer records an average SR Ra in μm by moving its stylus over the surface of a sample in a straight line. The roughness reading was noted on eight different points along the longitudinal axis of each sample and the average of the values was taken. The roughness of samples in as-built condition against each experimental run is given below in Table 4.

Table 4. Average SR values in As-built condition.

Run Order	WT (mm)	LP (W)	SS (mm/s)	HD (μm)	SR (μm)
1	1	320	900	105	11.575
2	3	320	900	105	8.985
3	1	380	900	105	8.873
4	3	380	900	105	12.210
5	2	350	730	80	12.156
6	2	350	1070	80	10.391
7	2	350	730	130	13.111
8	2	350	1070	130	9.563
9	1	350	900	80	11.012
10	3	350	900	80	11.610
11	1	350	900	130	13.816
12	3	350	900	130	10.146
13	2	320	730	105	9.538
14	2	380	730	105	9.993
15	2	320	1070	105	10.159
16	2	380	1070	105	10.477
17	1	350	730	105	10.240
18	3	350	730	105	12.682
19	1	350	1070	105	10.108
20	3	350	1070	105	9.587
21	2	320	900	80	11.086
22	2	380	900	80	10.945
23	2	320	900	130	11.818
24	2	380	900	130	9.182
25	2	350	900	105	9.727
26	2	350	900	105	10.869
27	2	350	900	105	10.253

The results indicate that a minimum value of surface roughness, i.e., Ra = 8.873 μm was recorded in the specimen of Run Order #3 having a wall thickness of 1.0 mm, laser power of 380 watts, scan speed of 900 mm/s, and hatch distance of 105 μm. The maximum value of SR (i.e., 13.816 μm) was seen in the specimen with run order #11. The corresponding values of wall thickness, laser power, scan speed, and hatch distance were 1.0 mm, 350 watts, 900 mm/s, and 130 μm, respectively.

3.2.1. Surface Roughness of Sand-Blasted Samples

One of the objectives of the experiment was to study the effects of one of the post-processing techniques (i.e., sand blasting) on the surface quality of the test specimens. As stated previously, the specimens were exposed to sand blasting at a pressure of 0.3 MPa for 4 min. A profilometer was used to measure the SR of specimens. The profilometer records average SR Ra in μm by moving its stylus over the surface of a sample in a straight line. The roughness reading was noted on eight different points along the longitudinal axis of each sample and the average of the values was taken. The average SR of samples after sand blasting against each experimental run is given below in Table 5.

Table 5. Average SR values after sand blasting.

Run Order	WT (mm)	LP (W)	SS (mm/s)	HD (µm)	SR (µm)
1	1	320	900	105	6.355
2	3	320	900	105	6.590
3	1	380	900	105	6.748
4	3	380	900	105	8.040
5	2	350	730	80	5.557
6	2	350	1070	80	5.337
7	2	350	730	130	5.442
8	2	350	1070	130	5.620
9	1	350	900	80	7.622
10	3	350	900	80	6.290
11	1	350	900	130	13.270
12	3	350	900	130	6.450
13	2	320	730	105	4.750
14	2	380	730	105	3.770
15	2	320	1070	105	4.200
16	2	380	1070	105	4.870
17	1	350	730	105	6.049
18	3	350	730	105	7.380
19	1	350	1070	105	5.947
20	3	350	1070	105	5.500
21	2	320	900	80	5.890
22	2	380	900	80	4.920
23	2	320	900	130	6.080
24	2	380	900	130	4.650
25	2	350	900	105	5.500
26	2	350	900	105	5.250
27	2	350	900	105	5.600

It can be observed from the Table 5 that the lowest reading of surface roughness (i.e., Ra = 3.77 µm) was obtained in the specimen of Run Order #14, having a wall thickness of 2.0 mm, laser power of 380 watts, scan speed of 730 mm/s, and hatch distance of 105 µm. The highest value of SR (i.e., 13.27 µm) was recorded in the specimen with run order #11. The corresponding values of wall thickness, laser power, scan speed, and hatch distance were 1.0 mm, 350 watts, 900 mm/s, and 130 µm, respectively. The graphical representation based on experimental data is also described below in Figure 5. This graph depicts the relationship between the surface roughness and the values of the perspective parameter.
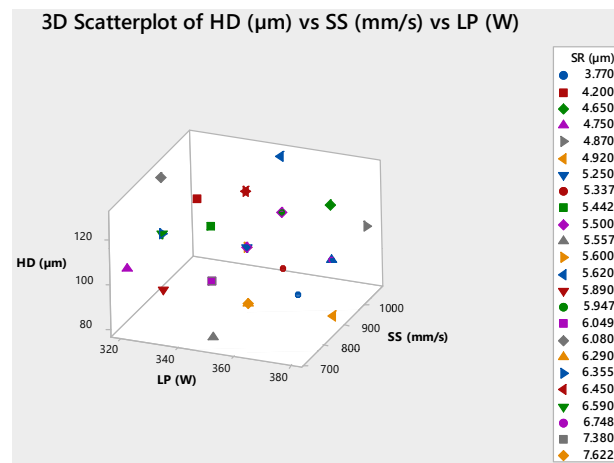

Figure 5. SR in respect to each of the parameters.

3.2.2. Dimensional Accuracy of the Samples

To study the effect of process parameters on the dimensional quality of the samples was also one of the objectives of the experimentation. The dimensional measurements (i.e., length and height) were measured using a digital vernier caliper. The design values for length and height were 55 mm and 12 mm, respectively, as given in Figure 2. The measurements of height were taken at five different points along the longitudinal axis, while length was recorded four times for every specimen. The average of these values was taken and are given in Table 6.

Table 6. Average values of the length and height of the samples.

Run Ord.	WT (mm)	LP (W)	SS (mm/s)	HD (μm)	Length (mm)	Height (mm)
1	1	320	900	105	54.818	12.025
2	3	320	900	105	54.920	12.030
3	1	380	900	105	54.805	12.068
4	3	380	900	105	54.933	12.050
5	2	350	730	80	54.958	12.020
6	2	350	1070	80	54.943	12.045
7	2	350	730	130	54.953	12.018
8	2	350	1070	130	54.920	12.055
9	1	350	900	80	54.795	12.073
10	3	350	900	80	54.940	12.060
11	1	350	900	130	54.895	12.033
12	3	350	900	130	54.965	12.070
13	2	320	730	105	54.883	12.025
14	2	380	730	105	54.905	12.055
15	2	320	1070	105	54.900	12.025
16	2	380	1070	105	54.920	12.035
17	1	350	730	105	54.848	11.998
18	3	350	730	105	54.950	12.010
19	1	350	1070	105	54.883	12.008
20	3	350	1070	105	54.888	12.020
21	2	320	900	80	54.920	12.028
22	2	380	900	80	54.935	12.060
23	2	320	900	130	54.888	12.078
24	2	380	900	130	54.918	12.073
25	2	350	900	105	54.913	12.065
26	2	350	900	105	54.983	12.043
27	2	350	900	105	54.963	12.038

It can be inferred from Table 6 that for the length of the specimens, the highest deviation from the design value occurred in run #9, yielding an average height of 54.795 mm at a wall thickness of 1.0 mm, laser power of 350 watts, scan speed of 900 mm/s, and hatch distance of 80 μm. The highest accuracy in the height was observed in run #26 with a recorded value of the average height being 54.983 mm. The corresponding values of wall thickness, laser power, scan speed and hatch distance were 2.0 mm, 350 watts, 900 mm/s, and 105 μm, respectively. For height of the specimens, the least precise value (i.e., 12.078 mm) was recorded in run #23, having process parameters of wall thickness = 2.0 mm, laser power = 320 watts, scan speed = 900 mm/s, and hatch distance = 130 μm. The highest accurate value of 11.998 mm was noted in run #17 with relevant values of wall thickness, laser power, scan speed, and hatch distance being 1.0 mm, 350 watts, 730 mm/s, and 105 μm, respectively. The summary of the graphical representation based on experimental results is given below. The Figure 6 describes the relationship between length and height and perception parameter values.
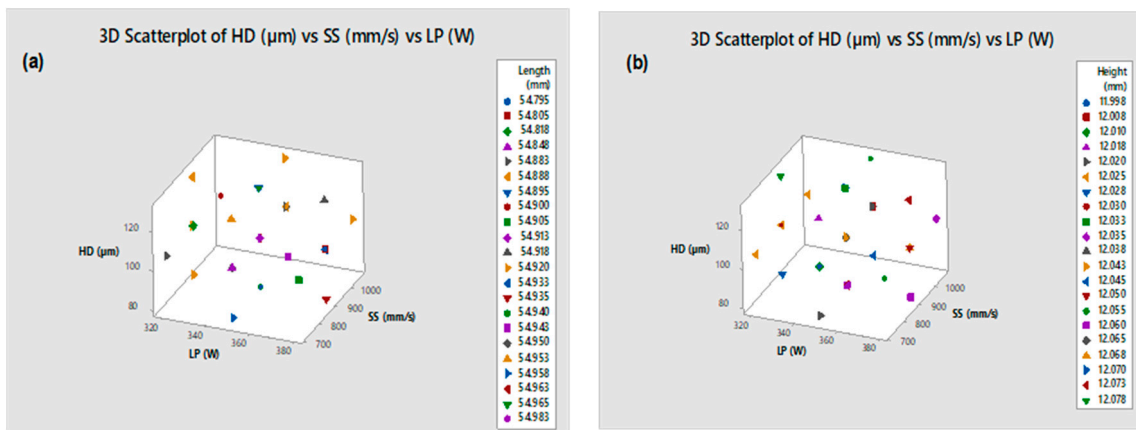
Figure 6. All plot parameter effects for (**a**) length and (**b**) height.

3.3. Surface Roughness

The main effects plot and interaction plot for SR are given in Figures 7 and 8, respectively.
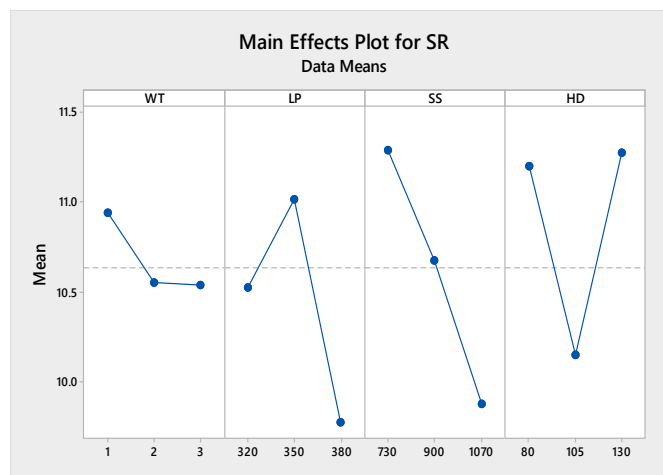

Figure 7. Main effects plot for SR.

Figure 8. Interaction plot for SR.

The main effect plot shows the mean of the response at every level of process parameter. Grand mean is displayed by drawing a horizontal line. The influence of process parameters is observed by the slope of the line which joins different levels of the process parameters. A steeper line indicates greater influence on response, while a line parallel to the grand mean displays a lesser effect on the response. It is clear from Figure 7 that scan speed had the greatest effect on surface roughness followed by laser power, while wall thickness had the least effect on the SR. The optimum value for surface roughness was attained at a scan speed of 900 mm/s, laser power of 380 W, and hatch distance of 105 μm.

The interaction among process parameters can be visualized by an interaction plot (Figure 8). In the plot, parallel lines point to no interaction. The interaction was very significant when lines moved away from being parallel. The plot indicates that a low value of SR was achieved at a high value of laser power and medium value of hatch distance. Significant interaction existed between hatch distance and wall thickness. There was a greater influence for hatch distance values of 80 μm and 130 μm at all values of wall thickness. There was also a significant interaction between the laser power of 380 W and wall thickness greater than 2.0 mm.

Regression Equation

The regression equation based on the chosen quadratic model is given below in Equation (1).

$$
\begin{aligned}
SR = {} & -92.5 - 4.40WT + 0.518LP + 0.0316SS + 0.124HD + 0.286WT*WT \\
& -0.000654LP*LP + 0.000002SS*SS + 0.001657HD*HD + 0.0327WT*LP- \\
& 0.00436WT*SS - 0.0427WT*HD - 0.000056LP*SS - 0.000832LP*HD \\
& -0.000105SS*HD
\end{aligned}
\tag{1}
$$

3.4. Dimensional Accuracy

3.4.1. Length of the Samples

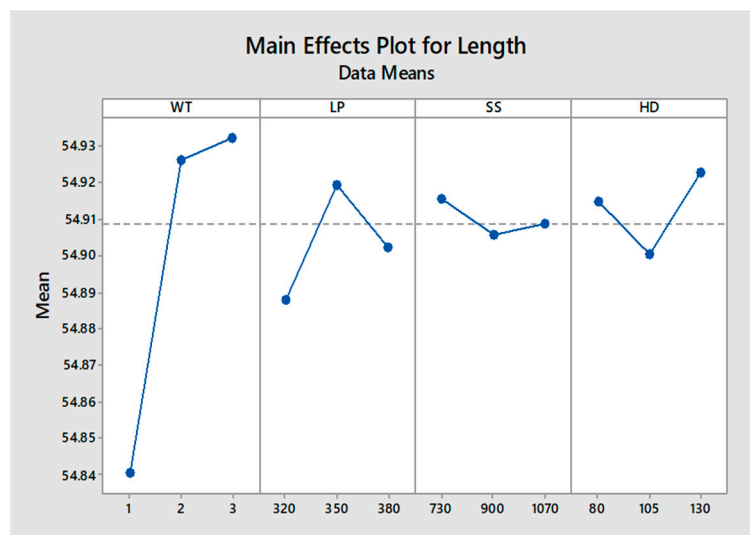The main effects plot for length was drawn and is given below in Figure 9.

Figure 9. Main effects plot for length.

It is clear from the figure above that wall thickness had the greatest effect on the dimensional accuracy of the samples in terms of length, while scan speed had the least effect on length. The most precise value for length was attained at a wall thickness of 3.0 mm, laser power of 350 W, scan speed of 730 mm/s, and hatch distance of 130 μm.

Regression Equation

The regression equation based on the chosen quadratic model is given below in Equation (2).

$$
\begin{aligned}
Length = {} & 49.04 + 0.380WT + 0.0279LP + 0.00110SS + 0.00118HD - 0.0498WT*WT \\
& -0.000041LP*LP - 0.000002HD*HD + 0.000208WT*LP \\
& -0.000143WT*SS - 0.000750WT*HD + 0.000005LP*HD \\
& -0.000001SS*HD
\end{aligned} \tag{2}
$$

3.4.2. Height of the Samples

The main effects plot for the height was drawn and is given below in Figure 10. It is clear from the figure above that laser power and scan speed had the greatest effect on the dimensional accuracy of the samples in terms of height. The most precise value for height was attained at a wall thickness of 1.0 mm, laser power of 320 W, scan speed of 730 mm/s, and hatch distance of 105 μm.
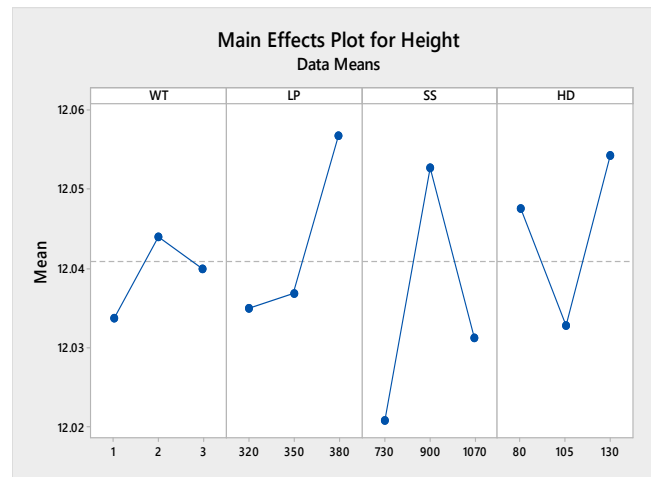

Figure 10. Main effects plot for height.

Regression Equation

The regression equation based on the chosen quadratic model is given below in Equation (3).

$$
\begin{aligned}
Height = {} & 11.27 + 0.051WT - 0.00071LP + 0.001854SS - 0.00125HD - 0.00875WT*WT \\
& +0.000005LP*LP - 0.000001SS*SS + 0.000020HD*HD \\
& -0.000187WT*LP + 0.000500WT*HD - 0.000001LP*SS \\
& -0.000013LP*HD + 0.000001SS*HD
\end{aligned} \tag{3}
$$

3.5. Selection of Optimum Process Parameters

Optimizing the process parameters for the responses was also one of the aims of the study. Minitab 17 was used to define the optimal process parameters to obtain better surface and dimensional qualities. The optimization plot and set of optimum SLM process parameters are given below in Figure 11.

The composite desirability is a single measure that combines the individual desirability of all the responses into a single measure. The figure below illustrates those responses were optimized and a composite desirability of 0.7472 was achieved. These optimized values of the response were obtained at a wall thickness of 2.7172 mm, laser power of 320 W, scan speed of 730 mm/s, and hatch distance of 94.1414 μm. Thus, these values combined make up a set of optimum process parameters against SR, length, and height as responses.
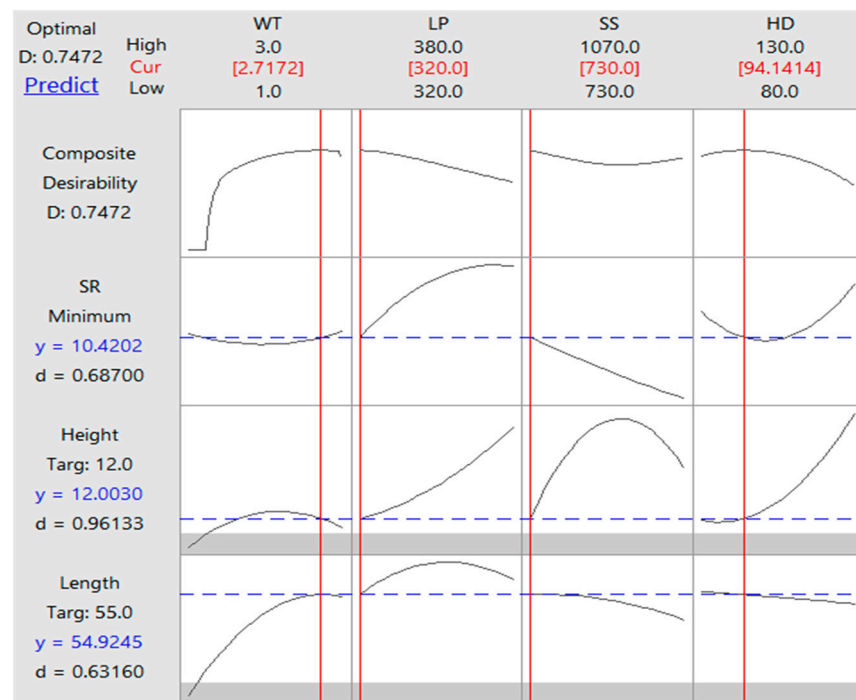
Figure 11. Optimization plot for SR, height, and length.

4. Conclusions

In this research work, the influence of SLM process parameters (i.e., wall thickness, laser power, scan speed, and hatch distance) on the surface and dimensional quality of AlSi10Mg specimens was studied. Response surface methodology was applied for DOE, analysis, prediction, and optimization purposes. ANOVA was applied to observe the effect of input factors on the responses. The conclusions made on the basis of the current study are listed below:

(1) With *p*-value and *F*-test value, wall thickness proved to have the most substantial influence on the length of the specimens in terms of dimensional accuracy. Length accuracy improved greatly when wall thickness varied from 1.0 to 2.0 mm. A further improvement in accuracy was observed when wall thickness varied from 2.0 to 3.0 mm;

(2) The response estimation model developed for length of the specimens was significant and yielded an R2 of 82.14%. This means that the developed model fits more than 80% of the response data;

(3) The values for SR, length, and height were predicted on the basis of respective regression equations developed with regression analysis of the responses. The SR, length, and height were predicted accurately with minimum error of 0.005%, 0.0%, and 0.002%, respectively, as compared to experimental values;

(4) The most precise value for height was achieved at a wall thickness of 1.0 mm, laser power of 320 W, scan speed of 730 mm/s, and hatch distance of 105 μm;

(5) The most accurate value for length was attained at a wall thickness of 3.0 mm, laser power of 350 W, scan speed of 730 mm/s, and hatch distance of 130 μm;

(6) Multi-objective optimization methods can be used to optimize different process parameters of the SLM process simultaneously;

(7) More statistical methods, such as the Taguchi method, artificial neural networks, fuzzy logic, genetic algorithms, and grey relational analysis, can be applied to analyze results.

Abbreviations

Nomenclature

ASTM	American Society for Testing and Materials
AM	Additive Manufacturing
SLM	Selective Laser Melting
EBM	Electron Beam Melting
DED	Directed Energy Deposition
BBD	Box–Behnken Design
RSM	Response Surface Methodology
SEM	Scanning Electron Microscope
3D	Three Dimensional
CAD	Computer-Aided Design
DOE	Design of Experiment
CCD	Central Composite Design
BBD	Box–Behnken Design
EIMSE	Expected Integrated Mean Squared Error
SEM	Scanning Electron Microscope
SR	Surface Roughness
WT	Wall Thickness
Auto Fab	Auto Fabrication
LP	Laser Power
SS	Scan Speed
HD	Hatch Distance

References

1. Kruth, J.-P.; Levy, G.; Klocke, F.; Childs, T. Consolidation phenomena in laser and powder-bed based layered manufacturing. *CIRP Ann.* **2007**, *56*, 730–759. [CrossRef]
2. Conner, B.P.; Manogharan, G.P.; Martof, A.N.; Rodomsky, L.M.; Rodomsky, C.M.; Jordan, D.C.; Limperos, J.W. Making sense of 3-D printing: Creating a map of additive manufacturing products and services. *Addit. Manuf.* **2014**, *1*, 64–76. [CrossRef]
3. Maamoun, A.H.; Elbestawi, M.; Dosbaeva, G.K.; Veldhuis, S.C. Thermal post-processing of AlSi10Mg parts produced by Selective Laser Melting using recycled powder. *Addit. Manuf.* **2018**, *21*, 234–247. [CrossRef]
4. Martin, J.H.; Yahata, B.D.; Hundley, J.M.; Mayer, J.A.; Schaedler, T.A.; Pollock, T.M. 3D printing of high-strength aluminum alloys. *Nature* **2017**, *549*, 365–369. [CrossRef]
5. Majeed, A.; Zhang, Y.F.; Lv, J.X.; Peng, T.; Waqar, S.; Atta, Z. Study the effect of heat treatment on the relative density of SLM built parts of AlSi10Mg alloy. In Proceedings of the 48th International Conference on Computers and Industrial Engineering (CIE 2018), Auckland, New Zealand, 2–5 December 2018.
6. Sing, S.L.; An, J.; Yeong, W.Y.; Wiria, F.E. Laser and electron-beam powder-bed additive manufacturing of metallic implants: A review on processes, materials and designs. *J. Orthop. Res.* **2016**, *34*, 369–385. [CrossRef]
7. Elahi, H.; Eugeni, M.; Gaudenzi, P. A review on mechanisms for piezoelectric-based energy harvesters. *Energies* **2018**, *11*, 1850. [CrossRef]
8. Elahi, H. The investigation on structural health monitoring of aerospace structures via piezoelectric aeroelastic energy harvesting. *Microsyst. Technol.* **2020**, 1–9. [CrossRef]
9. Elahi, H.; Eugeni, M.; Fune, F.; Lampani, L.; Mastroddi, F.; Paolo Romano, G.; Gaudenzi, P. Performance evaluation of a piezoelectric energy harvester based on flag-flutter. *Micromachines* **2020**, *11*, 933. [CrossRef]
10. Gibson, I.; Rosen, D.W.; Stucker, B. Design for Additive Manufacturing. In *Additive Manufacturing Technologies*; Springer Science and Business Media LLC: Berlin/Heidelberg, Germany, 2010; pp. 299–332.

11. Abbas, I.; Wang, Y.; Elahi, H.; Siddiqui, M.A.; Ullah, M.; Qayyum, F. Effect of MoSi2-Si3N4/SiC Multi-Layer Coating on the Oxidation Resistance of Carbon/Carbon Composites above 1770 K. *J. Compos. Sci.* **2020**, *4*, 86. [CrossRef]

12. Elahi, H.; Munir, K.; Eugeni, M.; Atek, S.; Gaudenzi, P. Energy Harvesting towards Self-Powered IoT Devices. *Energies* **2020**, *13*, 5528. [CrossRef]

13. Dadbakhsh, S.; Hao, L.; Jerrard, P.G.E.; Zhang, D.Z. Experimental investigation on selective laser melting behavior and processing windows of in situ reacted Al/Fe$_2$O$_3$ powder mixture. *Powder Technol.* **2012**, *231*, 112–121. [CrossRef]

14. Calignano, F.; Manfredi, D.; Ambrosio, E.P.; Iuliano, L.; Fino, P. Influence of process parameters on surface roughness of aluminum parts produced by DMLS. *Int. J. Adv. Manuf. Technol.* **2013**, *67*, 2743–2751. [CrossRef]

15. Leary, M. Surface roughness optimization for selective laser melting (SLM): Accommodating relevant and irrelevant surfaces. In *Laser Additive Manufacturing*; Elsevier: Amsterdam, The Netherlands, 2017; pp. 99–118.

16. Mohammadi, M.; Asgari, H. Achieving low surface roughness AlSi10Mg_200C parts using direct metal laser sintering. *Addit. Manuf.* **2018**, *20*, 23–32. [CrossRef]

17. Wang, L.-Z.; Wang, S.; Wu, J.-J. Experimental investigation on densification behavior and surface roughness of AlSi10Mg powders produced by selective laser melting. *Opt. Laser Technol.* **2017**, *96*, 88–96. [CrossRef]

18. Tian, Y.; Tomus, D.; Rometsch, P.; Wu, X. Influences of processing parameters on surface roughness of Hastelloy X produced by selective laser melting. *Addit. Manuf.* **2017**, *13*, 103–112. [CrossRef]

19. Rakesh, C.S.; Priyanka, N.; Jayaganthan, R.; Vasa, N.J. Effect of build atmosphere on the mechanical properties of AlSi10Mg produced by selective laser melting. *Mater. Today Proc.* **2018**, *5*, 17231–17238. [CrossRef]

20. Han, X.; Zhu, H.; Nie, X.; Wang, G.; Zeng, X. Investigation on Selective Laser Melting AlSi10Mg Cellular Lattice Strut: Molten Pool Morphology, Surface Roughness and Dimensional Accuracy. *Materials* **2018**, *11*, 392. [CrossRef] [PubMed]

21. Majeed, A.; Lv, J.; Peng, T. A framework for big data driven process analysis and optimization for additive manufacturing. *Rapid Prototyp. J.* **2019**, *25*, 308–321. [CrossRef]

22. Maamoun, A.H.; Xue, Y.F.; Elbestawi, M.A.; Veldhuis, S.C. The effect of selective laser melting process parameters on the microstructure and mechanical properties of Al6061 and AlSi10Mg alloys. *Materials* **2019**, *12*, 12. [CrossRef]

23. Sing, S.L.; Wiria, F.E.; Yeong, W.Y. Selective laser melting of lattice structures: A statistical approach to manufacturability and mechanical behavior. *Robot. Comput. Manuf.* **2018**, *49*, 170–180. [CrossRef]

24. Ghani, S.A.C.; Zakaria, M.H.; Harun, W.S.W.; Zaulkafilai, Z. Dimensional accuracy of internal cooling channel made by selective laser melting (SLM) And direct metal laser sintering (DMLS) processes in fabrication of internally cooled cutting tools. In *MATEC Web of Conferences*; EDP Sciences: Les Ulis, France, 2017.

25. Fateri, M.; Gebhardt, A.; Thuemmler, S.; Thurn, L. Experimental Investigation on Selective Laser Melting of Glass. *Phys. Procedia* **2014**, *56*, 357–364. [CrossRef]

26. Wang, R.-J.; Wang, L.; Zhao, L.; Liu, Z. Influence of process parameters on part shrinkage in SLS. *Int. J. Adv. Manuf. Technol.* **2006**, *33*, 498–504. [CrossRef]

27. Aboulkhair, N.T. *Additive Manufacture of an Aluminum Alloy: Processing, Microstructure, and Mechanical Properties*; University of Nottingham: Nottingham, UK, 2016.

28. Böckin, D.; Tillman, A.-M. Environmental assessment of additive manufacturing in the automotive industry. *J. Clean. Prod.* **2019**, *226*, 977–987. [CrossRef]

29. Allen, T.T. *Introduction to Engineering Statistics and Lean Six Sigma: Statistical Quality Control and Design of Experiments and Systems*; Springer: Berlin/Heidelberg, Germany, 2018.

30. Allen, T.T. *Introduction to Engineering Statistics and Six Sigmas': Statistical Quality Control and Design of Experiments and Systems*; Springer Science & Business Media: Berlin/Heidelberg, Germany, 2016.

31. Kruth, J.P.; Badrossamay, M.; Yasa, E.; Deckers, J.; Thijs, L.; Van Humbeeck, J. Part and material properties in selective laser melting of metals. In Proceedings of the 16th International Symposium on Electro machining (ISEM XVI), Shanghai, China, 19–23 April 2010.

32. Alrbaey, K.; Wimpenny, D.; Tosi, R.; Manning, W.; Moroz, A. On Optimization of Surface Roughness of Selective Laser Melted Stainless Steel Parts: A Statistical Study. *J. Mater. Eng. Perform.* **2014**, *23*, 2139–2148. [CrossRef]

33. Alsoufi, M.S.; Elsayed, A.E. Surface Roughness Quality and Dimensional Accuracy—A Comprehensive Analysis of 100% Infill Printed Parts Fabricated by a Personal/Desktop Cost-Effective FDM 3D Printer. *Mater. Sci. Appl.* **2018**, *9*, 11–40. [CrossRef]

34. Calignano, F.; Lorusso, M.; Pakkanen, J.; Trevisan, F.; Ambrosio, E.P.; Manfredi, D.; Fino, P. Investigation of accuracy and dimensional limits of part produced in aluminum alloy by selective laser melting. *Int. J. Adv. Manuf. Technol.* **2016**, *88*, 451–458. [CrossRef]

35. Majeed, A.; Zhang, Y.; Lv, J.; Peng, T.; Atta, Z.; Ahmed, A. Investigation of T4 and T6 heat treatment influences on relative density and porosity of AlSi10Mg alloy components manufactured by SLM. *Comput. Ind. Eng.* **2020**, *139*, 106194. [CrossRef]